

Phase Nanoengineering via Thermal Scanning Probe Lithography and Direct Laser Writing

Valerio Levati, Davide Girardi, Nicola Pellizzi, Matteo Panzeri, Matteo Vitali, Daniela Petti,* and Edoardo Albisetti*

Nanomaterials derive their electronic, magnetic, and optical properties from their specific nanostructure. In most cases, nanostructured materials and their properties are defined during the materials growth, and nanofabrication techniques, such as lithography, are employed subsequently for device fabrication. Herein, a perspective is presented on a different approach for creating nanomaterials and devices where, after growth, advanced nanofabrication techniques are used to directly nanostructure condensed matter systems, by inducing highly controlled, localized, and stable changes in the electronic, magnetic, or optical properties. Then, advantages, limitations, applications in materials science and technology are highlighted, and future perspectives are discussed.

new physics, and contributed to the birth and growth of research fields such as nanomagnetism and spintronics, nano-electronics, and nanophotonics. More recently, the rise of 2D materials^[2] such as graphene, where the films are up to a few atoms thick, and more in general of quantum materials,^[3] allowed to explore new exotic physical phenomena involving unconventional transport properties, and their applications.

Harnessing the electronic, magnetic, and optical properties of nanomaterials for realizing functional devices requires micro- and nanofabrication techniques,^[4] such as optical or electron-beam lithography. Conventionally,

1. Introduction


Nanomaterials acquire novel physical properties which derive from their specific nanostructure, or reduced dimensionality, and which can be markedly different from the properties of their bulk counterpart. For example, one of the most studied and applied classes of nanomaterials in condensed matter are thin solid films. They are characterized by extended lateral dimensions, and a low dimensionality in the vertical direction, which allows surface physics to dominate volume effects, and to be efficiently “stacked” in heterostructures composed of different materials, giving rise to new properties. The huge development of thin film growth techniques^[1] such as sputtering, molecular-beam epitaxy, pulsed laser deposition, or atomic layer deposition, following the semiconductor revolution in the 60s allowed to reach an astounding degree of control over the thickness, composition, crystalline structure, and coupling. This flexibility made thin films the most advanced materials playground for testing and studying

micro- and nanofabrication is used to “shape” materials, such as thin films, down to the nanometer scale by transferring geometric patterns via subtractive or additive processes. The majority of nanodevices are realized by combining thin film growth, which determines the properties of the material, with nanofabrication, which confers the functionality of the device by defining a suitable circuitry for probing or altering the desired physical properties.

In some cases though, the capabilities of nanofabrication can be used not only for device fabrication, but for inducing new physical properties in the material itself. One notable example is the one of optical metamaterials,^[5] where nanolithography is used to create periodic arrangements of nanostructures smaller than the light wavelength, which are seen by light as a uniform material, with different properties with respect to its uniform counterpart. In this sense, nanofabrication methodologies can be used to induce novel physical phenomena in a variety of materials systems, by locally modifying the geometry and structure with high nanoscale spatial resolution and precision.

In this paper, we discuss a recently developed methodology in condensed matter systems, called phase nanoengineering, providing an introduction to the concept and discussing the materials and techniques involved. Then, we give an overview of specific applications in the fields of magnetism, photonics, and electronics and provide an outlook over future improvements and applications.

V. Levati, D. Girardi, N. Pellizzi, M. Panzeri, M. Vitali, D. Petti, E. Albisetti
Department of Physics
Politecnico di Milano
Piazza Leonardo da Vinci 32, Milan 20133, Italy
E-mail: daniela.petti@polimi.it; edoardo.albisetti@polimi.it

 The ORCID identification number(s) for the author(s) of this article can be found under <https://doi.org/10.1002/admt.202300166>

© 2023 The Authors. Advanced Materials Technologies published by Wiley-VCH GmbH. This is an open access article under the terms of the Creative Commons Attribution License, which permits use, distribution and reproduction in any medium, provided the original work is properly cited.

DOI: 10.1002/admt.202300166

2. Phase Nanoengineering

Phase nanoengineering is based on directly inducing highly localized, tunable, and stable modifications to the physical

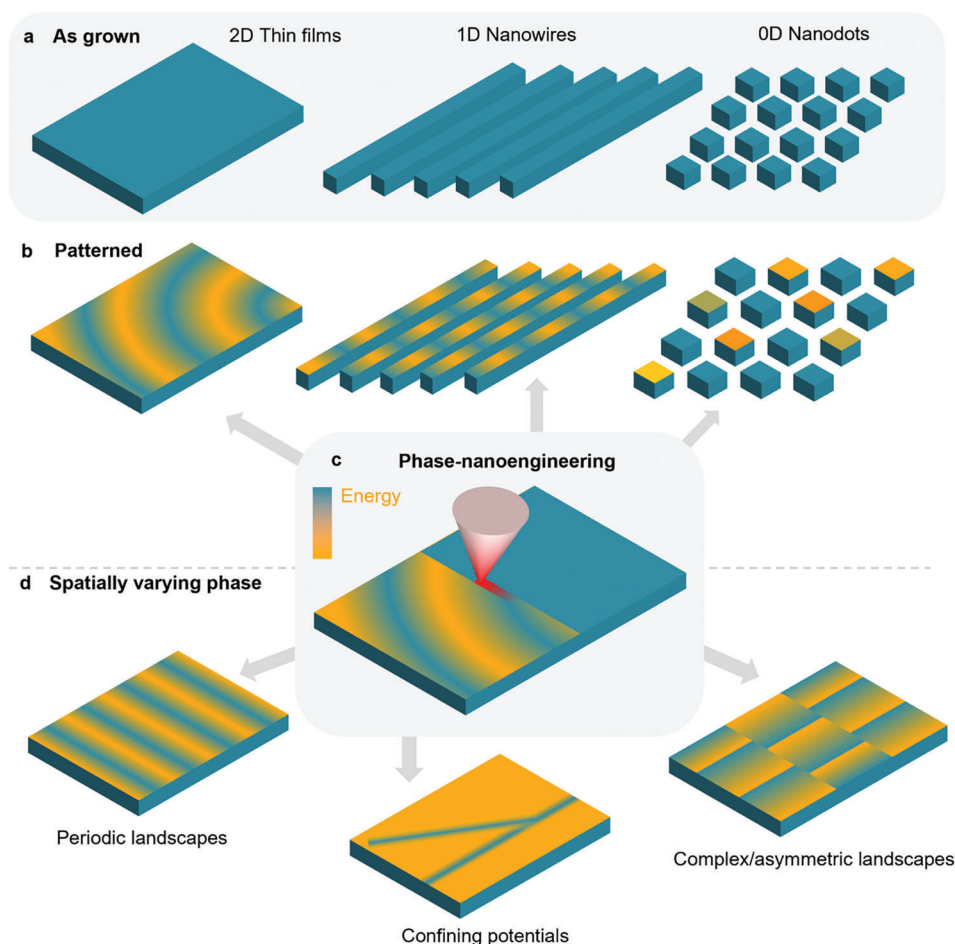


Figure 1. Schematic of phase nanoengineering. a) As grown 2D thin films, 1D nanowire arrays, and 0D arrays of nano-dots. They possess spatially uniform physical properties. b) Materials after the phase nanoengineering patterning corresponding to the 2D–1D–0D dimensionality above. c) The phase nanoengineering process is sketched. A highly localized energy source is scanned on the sample and produces point-by-point controlled modifications to the physical properties of the material. The color code indicates the “grayscale” energy landscape realized within the material. d) Examples of potential landscapes patterned via phase nanoengineering.

properties of materials via exposure with a highly localized energy source. The concept is shown in **Figure 1**. In panel a, after growth, nanomaterials are characterized by uniform physical properties across the plane. Nanomaterials with different dimensionalities are sketched in the case of 2D thin films, arrays of 1D nanowires, and arrays of 0D nanodots.

The phase nanoengineering methodology is sketched in **Figure 1c**, where a highly localized energy source irradiates point-by-point the material and induces controlled phase transitions, compositional, or structural modifications. By tuning the energy source while scanning the sample, it is possible to control point-by-point the degree of modification, creating “grayscale” profiles which in turn lead to highly controlled physical properties. This goes beyond the capabilities of most conventional nanofabrication methodologies, which in most cases allow for binary patterns characterized by the presence or absence of the material. The direct-writing process also has the advantage of not requiring to place the sample in contact with harsh chemicals, and of leaving completely untouched the non-patterned regions. This aspect is critical when dealing with sensitive materials, or in general ma-

terials which are not compatible with standard lithographic processes.

The material after the phase nanoengineering patterning process is shown in **Figure 1b**, where “grayscale” spatially-varying energy landscapes are stabilized, giving rise to new physical properties which allow to manipulate the characteristics and transport of particles (e.g., magnetic domain structure, electronic transport, spin currents) and waves (e.g., spin waves, plasmons, light). Depending on the geometry and properties of the energy landscape, with respect to the typical physical length-scales in play, widely different effects can be achieved. Some examples are reported in **Figure 1d**. Periodic energy landscapes, such as the 1D modulation shown in figure, can give rise to “grayscale” metamaterials such as magnonic^[6] or photonic^[7] crystals. Highly localized potentials on the other hand provide the basic building blocks for realizing nanoelectronic circuitry, for example, nanowires, nano-islands, gates. Similarly, in the case of waves, sharp property modulations, such as the refractive index in optics or the magnetic properties in magnonics allow confining effects, among which waveguiding,^[8] or tailored wave emission.^[9]

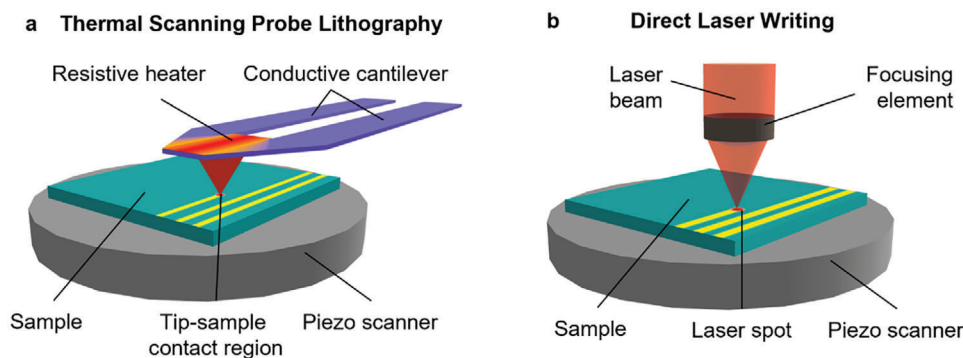


Figure 2. Working principles of a) tSPL and b) DLW. In both cases, the writing process occurs by moving the sample with respect to the energy source by means of a high precision positioner, such as a piezo-scanner. With tSPL, the energy stimulus is delivered to the material by the sharp heated AFM tip in contact with the sample, while for DLW a laser beam is focused on the sample surface.

Finally, more complex profiles can be envisioned for exploiting universal physical phenomena for the manipulation of transport. One intriguing example is the ratchet effect,^[10] which is associated to specifically engineered asymmetric energy landscapes, and allows unidirectional particle or quasiparticle transport and focusing, starting from symmetric external excitations.

3. Techniques

The capabilities of phase nanoengineering, in terms of the minimum feature size, or the achievable degree of properties modulation, are strictly related to the patterning technique employed in combination with the specific material. In the following, we will discuss two patterning techniques in the framework of phase nanoengineering: thermal scanning probe lithography^[11,12] (tSPL) and direct laser writing^[13] (DLW). Both allow a “clean” delivery of energy to the system, without the contamination associated to the presence of particles or charged beams such as electron or ion beams.

3.1. Thermal Scanning Probe Lithography

tSPL^[11,12] is a scanning probe lithography (SPL) technique that has proven reliable to directly pattern materials with a lateral resolution below 10 nm.^[14] tSPL's most widespread application is to pattern a polymeric resist by heating a probe tip around the resist sublimation temperature, causing the polymer to locally sublime.^[15,16] The resist can then be used as a mask for transferring patterns to the substrate. Aside from the resist sublimation, this intense, highly localized heat stimulus can be applied to a wide range of heat-activated processes, that include chemical modifications of the surface chemistry^[17,18] or physical transformations such as magnetic phase transitions promoting different alignment of magnetic dipoles,^[19] or local rearrangements of atoms that induce structural phase transitions.^[20] In this context, phase nanoengineering deals primarily with the direct modifications of the physical properties of materials.

tSPL is a maskless lithography technique, hence the pattern is written directly into the material without requiring a mask template, by following a sequential approach. While this reduces on

one side the maximum achievable throughput, which is currently comparable to electron-beam lithography for a single-tip,^[21] it allows on the other hand to change the patterning parameters pixel-by-pixel. Material properties can thus be modulated in a continuous scale (also known as grayscale patterning), rather than the “black and white” patterning of conventional lithographic techniques; this also includes quasi-3D patterning capabilities with nanoscale vertical resolution.^[22] The heat stimulus employed by tSPL, instead of charged beams employed by other techniques (like electron-beam lithography) avoids unwanted effects such as ionic implantation and trapped charges in the material and, consequently, a wider class of sensitive materials can be used. Moreover, since the interacting region of the material is of the order of the probe tip size, any problem that arises from proximity effects is strongly reduced.

As depicted in **Figure 2a**, in tSPL systems the thermal probe is mounted on an atomic force microscope (AFM)-like setup; a piezoelectric actuator is used to adjust the positioning of the probe with respect to the sample, with nanometric precision. Also, custom, dedicated electronics is used to control the heating of the AFM probe. The probe is a sharp AFM tip grown on a bendable, highly doped silicon cantilever with a resistive microheater incorporated above the tip. The resistive region is made of lightly doped silicon, thus when a current flows from the highly doped (conductive) cantilever into the resistive region, it will locally generate heat that diffuses toward the apex of the tip. The dimensions of the tip vary between 5 to 20 nm and the typical thermal constant for a silicon heater is as low as a few microseconds, allowing for extremely fast heating and cooling cycles, which leads to among the highest patterning throughput among scanning probe techniques.^[23] Another advantage of tSPL is the so-called in situ reading capability. By simply switching the thermal stimulus on and off, the tSPL system is capable of imaging the topography of the patterned surface without the need for time-consuming separate metrology phases. This integrated imaging provides instant information on the effectiveness of a patterning process and allows for real-time adjustment of the patterning parameters to better meet target criteria in a closed-loop lithography approach.^[24,25]

There are a few parameters that play a key role in successfully changing the properties of a material, and the temperature of the integrated heater is arguably the most important one. If it

is too low, no modifications are induced in the material, if it is too high, the material can be damaged. The heater temperature can be precisely set by controlling the applied electrical voltage, and can be measured by performing a temperature-voltage calibration before patterning.^[26] Noteworthy, the tip-sample interface temperature, which ultimately governs the patterning process, is always lower than the heater temperature, due to thermal dissipation through the sample, and depends on several parameters such as the tip geometry, contact area, sample roughness, sample thermal resistance.^[27]

Also, the sample's physical properties play a role in defining the patterning parameters. The thermal conductivity of the substrate and thickness of the films define the efficiency of the heat transport from tip to sample, so highly conducting samples will give rise to lower tip-sample interface temperatures, and thicker films will be less affected by the presence of the substrate.^[27]

The activation energy is also tightly related to the temperature, as it represents the energy barrier to overcome to trigger modifications in a material. Higher values of activation energy require higher temperatures, other than requiring longer times to complete the patterning.

The pixel heating time is the duration of the tip-sample contact time and determines the patterning speed. Together with temperature, it affects the patterning outcome. It can vary between a few and hundreds of microseconds and should be tuned according to the specific modification.

Finally, the tip size defines the heat transfer efficiency and the ultimate resolution of the process. Sharp tips, with diameters of only a few nanometers, lead to lower tip-sample contact temperatures, but allow for the best spatial resolution.

3.2. Direct Laser Writing

Direct laser writing (DLW) is a serial, mask-less optical beam lithography technique. Even if the spatial resolution is limited by diffraction (the minimum feature size is normally in the order of 1 μm , although with suitable modifications it is possible to achieve sub-wavelength resolution up to a few hundreds of nm^[28]), DLW technology has been investigated as a promising processing technology for inducing phase changes in materials due to its 3D processing capability and a wide variety of processing materials and applications.^[29] Inexpensive continuous wave (CW) lasers are frequently utilized for patterning materials at the micro/nanoscale in addition to more expensive femtosecond lasers for DLW. The laser power varies from a few milliwatts to several hundreds, while the wavelengths employed for laser emission are between 300 and 800 nm.^[29]

The general working principle behind DLW is a laser beam that is focused on a material, causing the material to change in the highly localized focal volume. The physical mechanisms producing the modification are several and are triggered by different linear and non-linear light absorption pathways.^[30]

The main components of a DLW system, sketched in Figure 2b, are a laser source that supplies the optical energy needed to modify a material, and a dedicated optical system that focuses the beam on the sample surface and controls the exposure time (for instance by means of a shutter). The material regions to be exposed are selected through a moveable stage that

holds the sample, and it is all controlled by a computer running specialized software connected to a motion controller for the moveable stage, and an observation and alignment subsystem.^[31]

To successfully nanopattern a material with DLW, few aspects need to be considered. First, the optical absorption properties of the sample at the laser wavelength are crucial in determining the required dose and patterning capabilities. Furthermore, the correct optical alignment of the laser beam is crucial and ensures the smallest possible beam spot. Any misalignment would severely degrade the maximum resolution of the process. The correct focusing of the laser beam spot on the sample surface is another key parameter, as an incorrect focusing would once again degrade the process resolution and reduce the power density delivered on the material, with the risk of failing in inducing phase modifications. Finally, the writing speed and exposure time are closely related and, together with the laser power, are among the most important parameters to determine the output.

3.3. Challenges and Outlook

Thermal scanning probe lithography and direct laser writing have great potential for phase nanoengineering due to their ability to directly modify materials without the contamination associated with other lithography methods. The use of thermal probes in tSPL and laser beams in DLW provides high resolution and versatility for creating complex nanostructures. Despite the advantages offered by these techniques, their limited throughput remains a significant challenge for high-volume industrial applications.

New approaches have been proposed to address this challenge, including the introduction of tip multiplexing for tSPL and beam shaping for DLW. The use of multi-tip approaches in tSPL employing arrays of cantilevers increases the throughput of the process since multiple features can be patterned at the same time. In ref. [32], the possibility of using heated cantilever arrays in an AFM system to perform parallel nanolithography is demonstrated. Similarly, in ref. [33], the parallelization of thermochemical scanning probe lithography (tcSPL) using an array of joule-heated cantilevers is demonstrated, achieving resolution down to sub-50 nm over areas of 500 \times 500 μm^2 and 3D patterning. More recently, a multi-tip approach was developed using an AFM system with a dual-tip or a four-tip probe to demonstrate the scalability of SPL systems for periodic patterning.^[34]

Beam-shaping techniques have been used to enhance the efficiency of the DLW process. For instance, spatial light modulators (SLM) can be used to shape the laser beam for patterning applications. In particular, precise patterning of complex structures can be achieved while significantly improving the throughput of laser patterning.^[35] In a different approach, holographic lithography, in particular laser interference lithography (LIL) can be used to shape laser beams for patterning applications. LIL is an effective technique for large-scale laser patterning as it allows for single-exposure patterning of periodical structures. In ref. [36], the authors employed a beam shaper that produces different beam energy profiles, such as a homogenous intensity profile useful for uniform patterning, a flat-top profile for 1D arrays, and a super-Gaussian intensity profile that can be used for grayscale periodic patterning.

Hybrid tSPL-DLW systems are a potential solution for improving throughput, as they can perform both tSPL for high-resolution patterning and DLW for larger features. Commercially available hybrid mix-and-match tools can perform tSPL and DLW using the same x - y piezostage to guarantee the correct alignment of features patterned with both processes.^[37] This effort for achieving high process efficiency and lateral resolution will require the development of new approaches and tools that will continue to drive progress in the field of nanofabrication.

4. Applications

In this section, we review some applications where tSPL and DLW are employed for the direct modification of materials via phase nanoengineering and other approaches, in the fields of magnetism, photonics, and nanoelectronics. In this framework, we discuss some of the most promising classes of materials, and how their direct patterning allowed to realize novel functionalities in micro-nanodevices.

4.1. Nanomagnetism and Spintronics

Magnetic materials, such as ferromagnets or antiferromagnets, possess a great fundamental and technological significance, and are at the basis of the field of spintronics, which aims to use the spin of electrons, instead of only their charge, for encoding and processing information. In this framework, numerous magnetic systems have been investigated for the development of devices based on spin textures, that is, micro- nanoscale non-uniform arrangements of the magnetization. Among these, current-driven domain-walls and skyrmions, magnetic textures stabilized in curved and 3D geometries, and nanostructures, such as nanoo oscillators have been intensively studied in the last decade.^[38] In view of conventional and unconventional computing applications and signal processing, therefore, finding new ways for manipulating the configuration of the magnetic moments, and more in general controlling the magnetic properties of the materials at the nanoscale is crucial.

Recently, phase nanoengineering has been proposed for creating magnetic nanopatterns on thin films with nanometric resolution. Specifically, highly localized heating can drive a wide range of processes leading to the creation of more energetically favorable states with modified properties, such as magnetic anisotropies or saturation magnetization, resulting in the local reorientation of the magnetic moments. In particular, using thermal scanning probe lithography (tSPL,^[8] Figure 3a) and direct laser writing (DLW) allows to directly control point-by-point the magnetic landscape with a “grayscale” profile and high degree of tunability, not feasible with standard lithographic techniques.

In this context, “thermally assisted magnetic scanning probe lithography” (tamSPL) is presented.^[19] Here, tSPL is used to reversibly nanopattern the desired magnetic configuration in a CoFeB (5 nm)/IrMn (7 nm) structure without altering the topography of the continuous film. The working principle of this technique consists in locally altering the exchange bias field^[39,40] in a ferromagnetic/antiferromagnetic bilayer by sweeping the hot tip of a scanning probe microscope in contact with the sample, in

presence of an external magnetic field. In order to locally modify the exchange bias of the system, the temperature of the tip is set above the blocking temperature T_B of the system, above which the exchange bias vanishes. While patterning, the external applied magnetic field switches the magnetization in the ferromagnet; as the tip is displaced, the heated region cools down and the exchange bias is locally re-set in the patterned region, which is observed as a shift in its hysteresis loop (Figure 3b). This technique allows to reach a high degree of tunability of the spin textures of magnetic films, without producing any sizeable change in the topography, chemistry or structural properties of the sample. The exchange bias strength can be modulated by changing the tip temperature and applied magnetic field during the nanopatterning process, creating a “grayscale” profile. The minimum feature size of the spin textures depends primarily on the magnetic properties of the system. For example, 250 nm wide stripe magnetic domains are stabilized by patterning single lines in an in-plane magnetized system,^[19] as reported in Figure 3c. Additionally, it is demonstrated a high degree of reversibility of the magnetic patterning procedure, providing full flexibility in writing, erasing, and rewriting the configuration of the magnetic anisotropy landscape in the nanopatterns (Figure 3c).

With this technique, a strategy for creating stable magnetic vortices and Bloch lines with controlled vorticity and chirality was developed,^[41] by tailoring vectorially the unidirectional anisotropy of the magnetic film with sub- μ m resolution. Figure 3d shows the MFM image of the controlled nucleation of vortex-antivortex pairs, where the direction of the magnetization of the domains has opposite chirality.

In view of applications, the engineering of the local exchange-bias field has also been proposed for designing a skyrmion-based spintronic device for memory and computing purposes.^[42] Through nanopatterning with tamSPL, the implementation of domain walls and potential wells could be used for the localization of skyrmions, for their annihilation and for enhancing their motion in magnetic racetracks.

tamSPL was also exploited for manipulating spin waves, in the field of magnonics.^[43–45] Spin waves are propagating perturbations in the orientation of spins, whose properties are strongly affected by the local orientation of the magnetization. By patterning the magnetization via tamSPL, it is therefore possible to control the spin-wave propagation and build reconfigurable nanoscale spin-wave circuits.^[8] To this goal, patterned spin textures, designed as magnonic waveguides, were used for channeling and steering the propagation of spin waves in a CoFeB (20 nm)/IrMn (10 nm) exchange-biased multilayer. In addition, optically inspired platforms were used for launching coherent spin-wave wavefronts in a synthetic antiferromagnetic (SAF) multilayer.^[9] As shown in Figure 3e, in this case the local exchange bias was modified via tamSPL for patterning spin textures acting as magnonic nanoantennas, and generating high-quality propagating spin wave wavefronts and robust spin-wave interference patterns.

The potential of tSPL has been also explored with regards to the heat-induced local rearrangement of atoms to facilitate the crystallization of amorphous materials by activating diffusion.^[11,12,14,46] In this framework, it has been demonstrated the possibility of systematically creating, in a non-magnetic thin film of CoFe₂O₄ gel, crystallized nanodisks with ferromagnetic

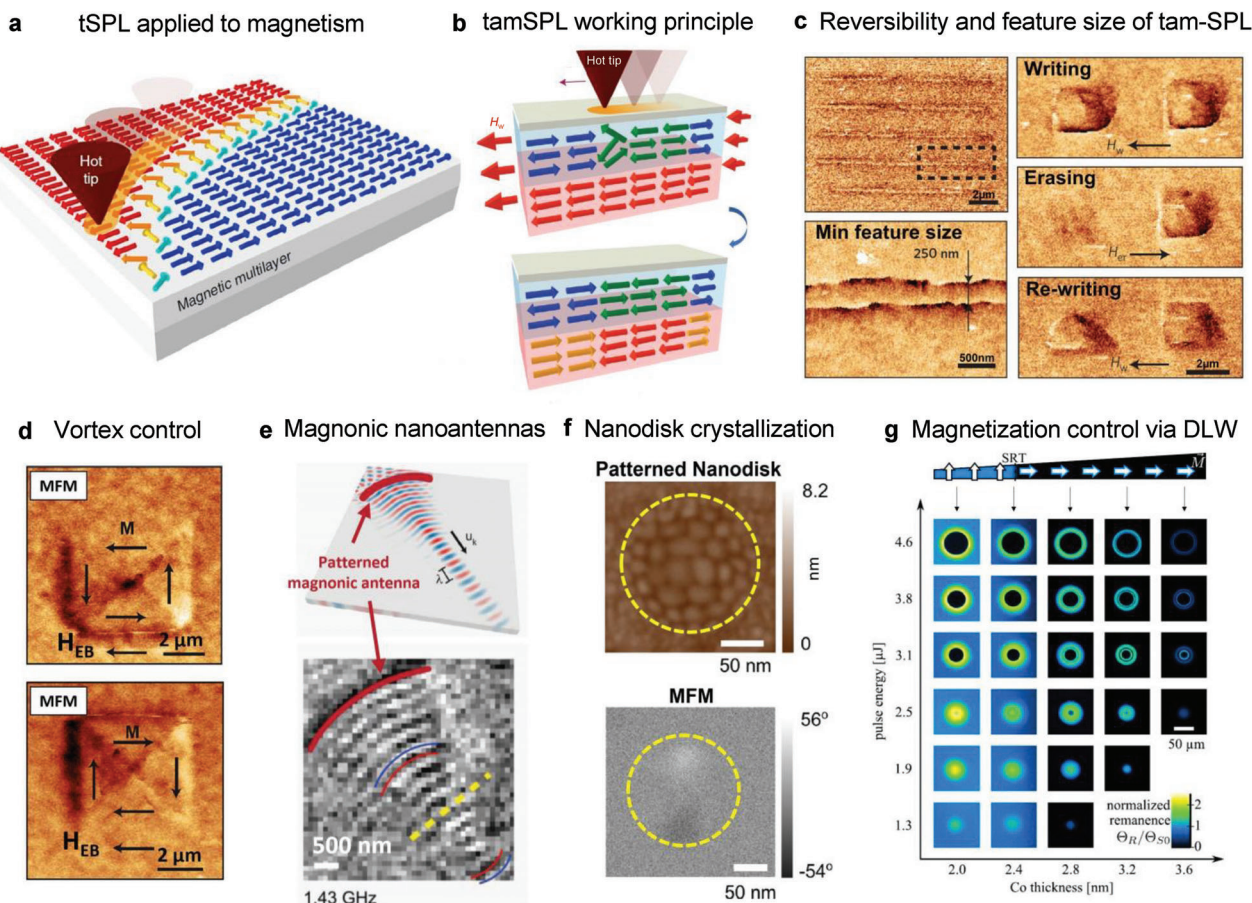


Figure 3. Applications in nanomagnetism and spintronics. a) Sketch of the thermal scanning probe lithography technique applied to magnetism, allowing the local reorientation of the magnetic moments. Adapted with permission.^[8] Copyright 2018, Springer Nature. b) Working principle of the thermally assisted magnetic scanning probe lithography (tamSPL) for the local engineering of the exchange bias field in ferromagnet/antiferromagnet multilayers and formation of patterns with tunable direction of the magnetization. Adapted with permission.^[19] Copyright 2016, Springer Nature. c) MFM images of stripe domains written via tamSPL (left) and for the demonstration of the reversibility of the technique. Different magnetic domains are written, erased and rewritten in the magnetic film (right). Adapted with permission.^[19] Copyright 2016, Springer Nature. d) MFM images showing the stabilization of vortex-antivortex pairs through tamSPL nanopatterning and the control of magnetic domains with opposite vorticity and chirality. Adapted with permission.^[41] Copyright 2018, AIP Publishing. e) Patterning of magnonic nanoantennas via tamSPL in a synthetic antiferromagnetic (SAF) structure, for the generation of propagating spin waves, observed via scanning transmission X-ray microscopy. Adapted with permission.^[9] Copyright 2020, Wiley-VCH GmbH. f) Creation of crystallized nanodisks with ferromagnetic vortex from a non-magnetic thin film of CoFe_2O_4 gel. On the top, AFM image of the crystallized nanodisk after the patterning procedure via tSPL. On the bottom, MFM image of the nanodisk, confirming the formation of the vortex. Adapted with permission.^[47] Copyright 2018, Elsevier. g) Analysis of the change in the anisotropy axis on the Co film in a Pt/Co/Pt multilayer, as a function of the film thickness and laser power. Low-energy laser pulses stabilize an out-of-plane magnetization, while higher energy laser pulses lead to predominant in-plane magnetization for all thicknesses. Adapted with permission.^[50] Copyright 2014, AIP Publishing.

vortex domains by performing a local annealing with a heated AFM tip at 700°C .^[47] By varying the heating times between 15 and 150 s, the resulting diameters of the nanodisks increased from 150 to 300 nm. In the AFM images shown in Figure 3f, it is possible to recognize the outline of the crystallized nanodisk, after the local annealing procedure on the non-magnetic gel film, and the resulting ferromagnetic vortex domain.

Besides thermal scanning probe lithography, direct laser writing (DLW) has been proven as a powerful and multifunctional localized energy source for applications in magnetism. Historically, the interaction of light with magnetic films has been deeply investigated in the framework of all-optical magnetization switching experiments, where light is used for reversing the magnetization

direction in ferromagnetic or ferrimagnetic thin films.^[48] However, in this case, light produces only temporary modifications to the magnetic properties, which revert back to the initial values after the magnetization switching, when the beam is switched-off. Permanent laser-induced changes are exploited instead in ref. [49], where laser-induced local modification of the magnetic landscape in a thin Fe–Cr film with no long-range magnetic order is achieved, with the formation of ferromagnetic regions with well-defined direction of the easy magnetic axis.

A different approach was employed in refs. [50,51], demonstrating the irreversible modification of the magnetic properties and the improvement of the magneto-optical signal in thin Pt/Co/Pt and Au/Co/Au stacks by local irradiation with single

femtosecond laser pulses. The effects were analyzed as a function of the Co thickness and of the laser power, whose fine tuning allows to manipulate in a “grayscale” fashion the orientation of the magnetization by changing direction of the anisotropy axis. Specifically, as reported in Figure 3g, low-energy laser pulses favor the stabilization of a strong out-of-plane magnetization, either improving the already dominant out-of-plane anisotropy axis for small thicknesses or shifting it from in-plane to out-of-plane above a certain thickness threshold. On the other hand, higher energy laser pulses lead to predominant in-plane magnetization for all thicknesses.

Laser irradiation has also been exploited in magnonics. In ref. [52], the spatially shaped thermal profiles induced by laser irradiation induce temporary localized periodic variations in the magnetic properties of materials for the realization of magnonic crystals. In magnonics, YIG films are among the most studied,^[53] and the control of the spin-wave transmission characteristic with the formation of tunable bandgaps is a key aspect for achieving new schemes of spin-wave based computing. By fabricating periodic antidot structures by laser ablation of the film surface,^[54] it is possible to finely tune and modulate the YIG spin-wave resonance spectra, with the formation of an additional peak depending on the periodicity of the antidots.

In this framework, a wide range of applications of phase nanoengineering in the field of magnetism can be envisioned. For example, in the field of magnonics, the local modification of the magnetic properties of materials with these techniques opens up the possibility of using inverse-design for the creation of the building blocks for Boolean and neuromorphic computing, similarly to what has been proposed in refs. [55,56]. The fabrication and tuning via phase nanoengineering of artificial spin ices (ASI), frustrated systems built up by interacting single domain nanomagnets arranged in specific geometries, hold promises for different applications.^[57] For example, their tunable dynamics can be employed in nano-oscillators or magnonic crystals^[58] or their reconfigurability can be exploited in reservoir computing.^[59] Furthermore, in refs. [60,61], skyrmion-based logic devices have been proposed by locally modifying the anisotropy properties in magnetic films. In addition, phase nanoengineering could play a major role in the patterning and creation of magnetic racetracks for domain wall logic.^[62] Finally, the tuning of the properties of the recently discovered class of magnetic 2D materials^[63] via phase nanoengineering holds great potential in view of spintronic and spin-caloritronic applications,^[64] such as spin quantum dots, spin field-effect transistors, magnetic tunneling junctions, and spin valves, spin orbit devices, and sensors or generators based on spin Seebeck effect.

Technique-wise, combining the high-resolution patterning and nanometer-accuracy of tamSPL with laser writing would enable innovative hybrid nanolithography approaches.^[46] This mix-and-match capability will become useful for the local manipulation and fine tuning of the magnetic properties in new innovative magnetic metamaterials.

4.2. Photonics with Phase Change Materials

The possibilities related to the direct manipulation of the optical properties have been widely studied and applied in the past

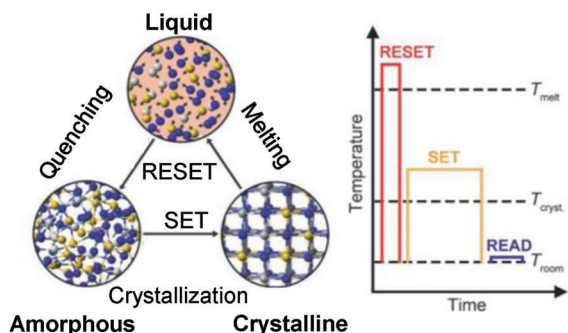
decades. For example, the use of fs-laser micromachining for the direct fabrication of 3D photonic devices in a variety of transparent optical materials is well established.^[65,66] Fs-laser micromachining is based on the ability to induce non-linear absorption in transparent media such as glass. This phenomenon occurs when a small volume of the material is subjected to a high intensity field for a short time in the 10–100 fs range. This energy transfer can cause changes in phase or structure, which lead to permanent changes to the refractive index, which in turn can be used for fabricating integrated devices such as waveguides and circuits.

Another promising research area is the direct processing of phase change materials (PCMs). In this section, we will primarily focus on PCMs, due to their versatility and importance across various fields. The PCMs treated in this perspective are those belonging to the class of chalcogenides, alloys containing chemical elements of group 16 of the periodic table such as sulfur (S), selenium (Se) and tellurium (Te), which have advantages that are extremely important for all-optical devices. The most important are low switching energy, high switching speeds and high thermal stability.^[67] PCMs possess two configurations stable at room temperature, one with a short-range atomic order, the amorphous state, and the other with a long-range atomic order, the crystalline one. The two states have significantly different electrical and photonic characteristics. Conceptually, the transition between the two phases takes place as described in **Figure 4a**. These materials have two transition temperatures, the first one is that of crystallization, beyond which the phenomena of atomic reorganization toward the crystalline state are active. The second one is that of melting, beyond which the transition to the liquid phase occurs, with consequent destruction of the crystalline order. Using short laser pulses or via the joule effect of a coupled resistance, starting from the amorphous state, the material is heated above the crystallization temperature for a time suitable for the formation of the crystalline structure (SET operation). The amorphization process occurs by heating the material above the melting temperature followed by rapid cooling which freezes the material in a disordered state (RESET operation).^[68]

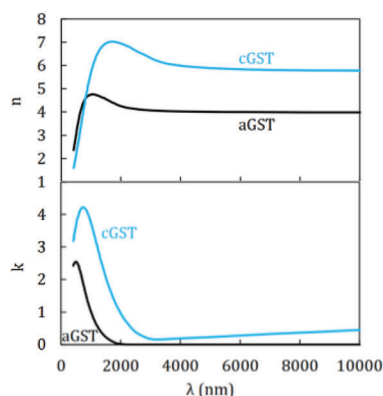
In order to exploit these peculiar mechanisms to obtain easily reconfigurable devices in the UV to IR spectral range, a multitude of alloyed chalcogenides (ChG) containing germanium, gallium and antimony have been identified in recent years. In particular, $\text{Ge}_2\text{Sb}_2\text{Te}_5$ (GST), GeTe , $\text{Ge}_2\text{Sb}_2\text{Se}_4\text{Te}_1$ (GSST), Sb_2S_3 (SbS), and Sb_2Te_3 are the most promising.^[69]

The optical properties of PCMs can be well visualized through the analysis of the refractive index (n) and the extinction coefficient (k) spectra, which represent fundamental information for the design of photonic devices. A very significant feature is the reversible n and k variation of the GTS in the two phases, as shown in **Figure 4b**. In the amorphous phase (aGTS), n exhibits a peak of $n = 4.7$ at $\lambda = 990$ nm which then stabilizes at about 4 for a wavelength between 2 and 10 μm . In the crystalline phase (cGTS), the peak is found at 1650 nm and is equal to 7.1, while the plateau is reached after 4000 nm with a value around 6. Significant variations are also present in the extinction coefficient of the material, where it is possible to observe a red shift of the plasmon resonance peak, from 450 nm (aGST) to 660 nm (cGTS).^[70] Such important variations of n and k are evidently reflected in the transmission, reflection, and absorption properties which, depending

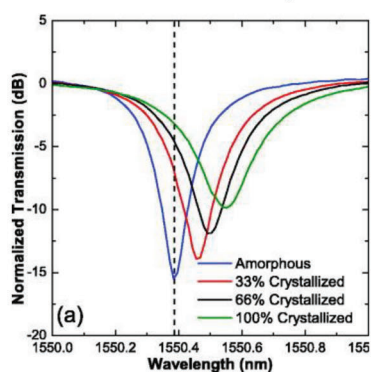
a PCMs operating principle



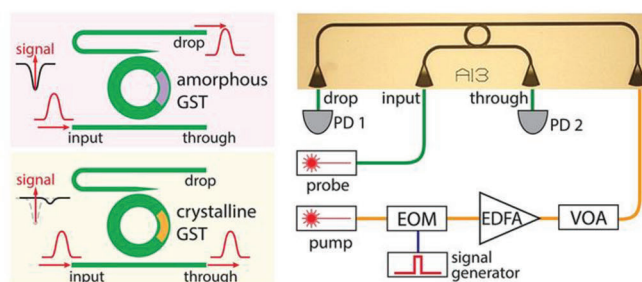
b GST optical properties variation



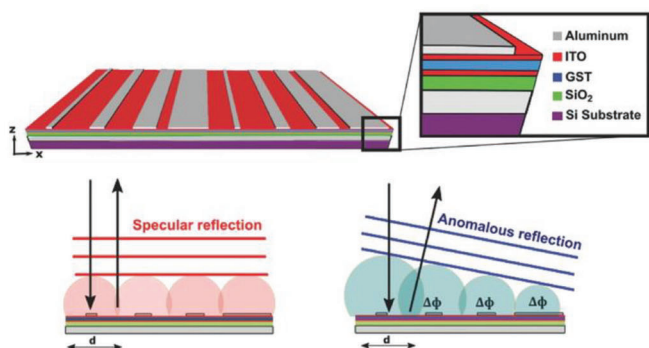
c GST transmission spectrum



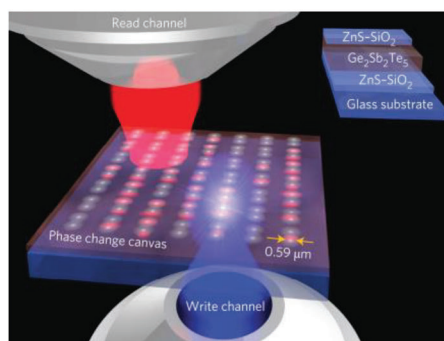
d Integrated Photonic Switch



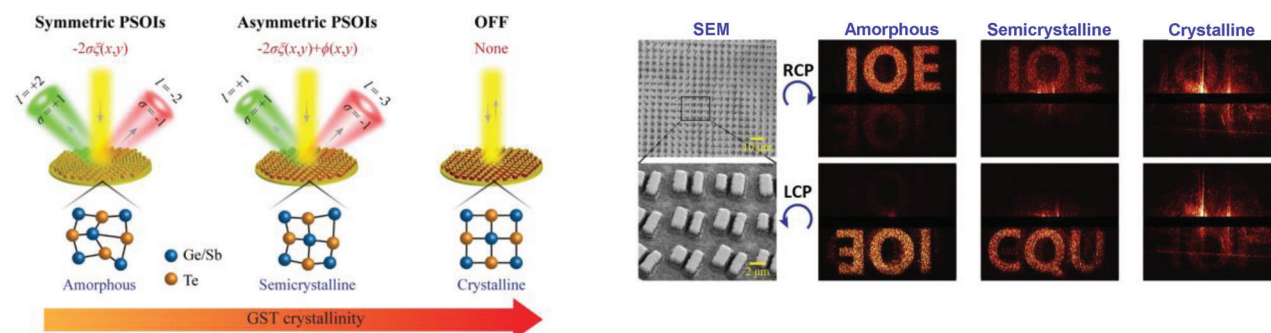
e Reconfigurable beam-steering device



f PCM writing and reading process via DLW



g Encryption of information in PCM via PSOs



on the phase imposed on the material, can be exploited in the field of data storage, computation, and to develop easily reconfigurable optical devices.

The possibility of wavelength multiplexing, low power consumption, ultrahigh information-processing speed, and wide frequency bandwidth offers multiple advantages in the development of all-optical computing devices compared to silicon technology. In this sense, several solutions for the photonic integrated circuits have been developed in the last decade.^[71]

The first optical reversible device that exploits the reflectance variation is represented by rewritable optical media (e.g., CD, DVD), which through the use of high intensity laser beam is able to induced state of high (bit 1) and low (bit 0) reflectance, while using a lower optical intensity it is possible to read the memorized state.^[72] In recent years, sub-wavelength structures have been explored to create waveguides incorporating PCMs along their path or coupling with PCM micro-ring resonators in order to process photonic signals. Because the complex propagation constant of the waveguide mode depends on the phase state of the PCMs, the resonant frequency and the transmission spectrum of the device are also strongly affected upon transition from the amorphous to the crystalline phase. This is the basis for information storage and elaboration in phase-sensitive photonic devices. Furthermore, it is also possible to exploit different degrees of crystallization to have a continuous variation of the photonic properties^[73] (Figure 4c). A device example that takes full advantage of this approach is shown in Figure 4d where a low-loss integrated photonic switch is achieved.^[74] The strategy adopted was to exploit a pump system to set the degree of crystallization of the GSTs integrated in a micro-resonator, and a probe laser that can be switched between a through port or a drop port in an arbitrary manner. This solution is well suited to photonic switching networks, which are very important for the development of all-optical computing devices. Through this approach, it is possible to realize programmable optical logic devices,^[75] all-photonic memory elements,^[76] multimode photonic computing cores,^[77] and neuromorphic photonic computing devices.^[78,79]

Another sector in which the PCMs use is promising is that of optical elements. In this case, the reconfiguration strategies of the optical properties of the elements essentially follow two methods: mechanically modifying the geometrical features of the nanostructure or using materials with controllable refractive in-

stances. The first way is based on the creation of photonic resonators in which it is possible to change the plasmon response of the nanostructures by acting on parameters such as distance and size. This strategy, due to the mechanical stress, significantly limits the tuning speed.^[80] For the second approach, liquid crystals have historically been used, where it is possible to obtain an effective change of the refractive index via external stimuli. Nevertheless, these are limited in modulation speed (milliseconds to microseconds) and tunability due to the small change in refractive index and slow switching speed.^[81] The ability to significantly modulate n and k of a material offers the possibility of realizing tuned optical elements through PCMs metasurfaces. Very interesting examples are varifocal metalenses,^[82] nanopixel displays,^[83,84] tunable absorber cavities,^[85] planar wavelength multiplexing focusing devices.^[86] In Figure 4e, it is shown the principle of operation of a reconfigurable beam steering^[87] working in the infrared region. The device is composed of a multilayer stack, in which the active optical components are a combination of periodical arrays of plasmonic structures (with different dimensions) and GST layer. The heat switch in this device is activated through a transparent ITO layer heated by the joule effect. When the crystalline state is set, the structure behaves as a mirror, and the reflected light follows conventional Snell reflection laws (the angle of reflection is equal to the angle of incidence). The device radically changes behavior when the PCM level is set to the amorphous state. In this configuration the plasmonic structures couple differently with the new value of the refractive index giving rise to a phase shift which varies along the surface as a function of the structure size (Figure 4e). This particular phase-response results in a constructive interference in a direction different to that of specular reflection, giving rise to the so-called anomalous reflection. This application demonstrates how combining PCMs with plasmon metasurfaces represents a promising strategy for realizing reconfigurable nanostructured optical devices.

A crucial aspect that has emerged in recent years is the possibility of exploiting the presence of intermediate states between the crystalline and amorphous phases in PCMs.^[88] This characteristic is achieved thanks to the possibility of making the amorphous and crystalline state coexist, being able to vary their ratio. Important applications have been implemented for the storage of encrypted information^[89] and in the realization of metasurfaces with modulable non-linear optical response.^[90] In

Figure 4. Applications in photonics. a) Working principle of phase change materials. Voltage or laser pulses heat up PCMs to different temperatures, either above the melting temperature (T_{melt}) or in between the crystallization temperature (T_{cryst}) and the melting temperature. Adapted with permission.^[68] Copyright 2020, Springer Nature. b) Optical properties of aGST and cGST as calculated using the dielectric functions. The shift in the field-enhancement spectral band is due to the larger refractive index (n) of the crystalline phase. Adapted with permission.^[70] Copyright 2016, American Chemical Society. c) Evolution of the transmission spectrum during crystallization and amorphization of the GST film. Adapted with permission.^[73] Copyright 2013, AIP Publishing. d) Optical switch operation principle and measurement scheme. Left: when the GST is in the amorphous phase, the signal resonantly couples into the microring and outputs from the drop port with a very low loss. When the GST is in the crystalline phase, the signal is decoupled from the microring and outputs directly from the through port to avoid any optical loss. Right: pulses from a pump laser are used to optically control the phase transition of the GST, thereby switching the output of the probe laser between the through and drop ports. Adapted with permission.^[74] Copyright 2019, American Chemical Society. e) Reconfigurable phase change beam-steering device design. Top: structure and materials of the device. Bottom: Huygens principle showing the wave front reconstruction under normal incidence when the GST layer is in the crystalline, and amorphous states. Adapted with permission.^[87] Copyright 2018, Wiley-VCH GmbH. f) The write channel uses high intensity laser pulses to induce a refractive index change into the GST film, which is then revealed by the read channel using a low intensity laser. Adapted with permission.^[86] Copyright 2020, Wiley-VCH GmbH. g) Left: Schematic of the different PSOs obtained as a function of the written crystalline state. Right: structured metasurface containing encrypted information (SEM images on the left). On the right, the different meta-holograms obtained with right (RCP) or left (LCP) circularly polarized light and the different crystalline state of the material. Each combination returns correct, misleading, or null information. Adapted with permission.^[89] Copyright 2015, Springer Nature.

particular, in ref. [89] a metal–dielectric–metal metasurface exploits the coupling between spin and orbital angular momenta of photons, that is, photonic spin–orbit interactions (PSOIs). Figure 4g shows a schematic of the different PSOI mechanisms induced by the diverse crystalline states of the GST, where the symmetric (asymmetric) PSOIs enables the joint (independent) tuning of the right/left circular polarization. This property has been used to store encrypted information in metaholograms, readable only if the correct decryption key, that is, the appropriate phase state of GST achievable at a given temperature, is known. On the contrary, if the reading status is wrong, misleading information or noise are returned (Figure 4g, right panel).

Finally, Figure 4f shows a possible writing and reading mechanism of reversible structures created with PCMs: femtosecond pulses write complex refractive index profiles, by changing continuously the PCM phase from amorphous to crystalline. A read channel checks the different optical components.

In conclusion, direct engineering of the optical properties of PCMs is an extremely active field, and PCMs are well suited to be the future platforms for all-optical devices. Although the mentioned applications are to be considered still at the prototype stage, characteristics such as wavelength multiplexing, low power consumption, ultrahigh information-processing speed, and wide frequency bandwidth are usually required in any technology that is a candidate for silicon successor. All these aspects, combined with the possibility of finely tuning the degree of crystallinity and thus obtaining intermediate or superimposition of different states, make them very promising materials in the field of computing and anti-counterfeiting. Furthermore, the demonstration of how these materials can be integrated into silicon-based devices ensures their high scalability and integrability into currently used industrial processes.

4.3. Electronics

Thermal scanning probe lithography and direct laser writing can be effectively employed to manipulate the electronic properties in a wide range of systems, and to fabricate electronic devices from materials that are challenging for conventional nanofabrication techniques. In this regard, the most widespread examples of phase-dependent properties can be observed in phase change materials,^[91,92] such as $\text{Ge}_2\text{Sb}_2\text{Te}_5$, where the amorphous and crystalline phases show different electrical resistivity, and in 2D semiconductors,^[93] such as graphene or transition metal dichalcogenides (TMDC) monolayers,^[94] which are as promising for optical and electronic applications, as difficult to deal with when fabricating actual devices.

In recent years, PCMs have been extensively studied for the development of reconfigurable electronic devices for storage and computing applications. In such materials, it is well known that heat-induced phase transformations produce sizeable changes in their electronic transport properties; accordingly, localized heating provided by tSPL and DLW represent a remarkable tunable technique for addressing micro- and nanoscale fabrication of phase change devices.^[95] In particular, it has been proposed the concept of thermal data recording in GST, as depicted in **Figure 5a**, where amorphization and crystallization, and thus switching between high and low resistivity state, occur after in-

direct heating from a tip irradiated by a pulsed laser over an area smaller than 50 nm, instead of a conventional change induced by joule effect.^[96] Besides the widely studied GST, other phase change materials, and also geometries and patterning parameters have been investigated, such as λ -dependent DLW on $\text{Ag}_8\text{In}_{14}\text{Sb}_{55}\text{Te}_{23}$ ^[97] and selective reversible crystallization of $\text{Cu}_{77}\text{Ni}_6\text{Sn}_{10}\text{P}_7$ ribbons.^[98] A noteworthy application is the fabrication of monolithic serial interconnection of solar cells made of $\text{Cu}(\text{In}_x, \text{Ga}_{1-x})\text{Se}_2$ chalcopyrite through the laser tuning of the electrical conductivity (Figure 5b), which turns out to be higher in exposed regions due to selective vaporization entailing larger fraction of copper, gallium, and zinc.^[99]

Since the discovery of graphene in 2004, the physics and applications of 2D materials have gained more and more interest. However, despite their unique transport properties, for example, high mobility, their implementation in real electronic devices is prevented by patterning difficulties, such as the fabrication of metallic ohmic contacts on top of them with standard processes. In this framework, it has been shown that tSPL can effectively be used to directly pattern graphene-based systems by inducing thermally-driven chemical reactions. In fact, tSPL provides a way to tune the electrical properties of graphene oxide (GO) with nanoscopic resolution (below 15 nm) by local thermal reduction.^[100,101] The change in resistivity can be observed in Figure 5c where a conductive-AFM measurement of the system together with a schematic of the apparatus are shown. Reduced GO is indeed about 10^4 times more conductive than unpatterned GO, making this technique a viable route for the development of future flexible graphene electronics. Moreover, a heated AFM probe was used to fabricate nanoribbons (GNRs) as narrow as 40 nm by locally converting highly insulating graphene fluoride (GF); such structures showed a resistivity only ten times larger than pristine sheet graphene.^[102]

Furthermore, tSPL and DLW have been proposed for changing the structural phases of TMDCs; the most studied example being the 2H-to-1T' phase transition in MoTe_2 , from the semi-conducting hexagonal (2H) phase to the metallic monoclinic one (1T').^[103] Upon laser irradiation it is therefore possible to precisely control the layer-by-layer thinning and phase engineering of few-layer MoTe_2 ,^[104] allowing the formation of an ohmic homojunction contact.^[105,106] Both the concept and the experimental results are presented in Figure 5d. In order to address the versatility of the technique, it is worthwhile to report that similar results have been obtained for the 1T/1T' phase transition in MoS_2 ,^[107] thence providing a viable route toward 2D TMDCs based electronics. Another strategy for directly engineering transport in 2D materials uses tSPL for creating controlled defect concentrations, which in turn lead to localized p-type or n-type doping, depending on the atmospheric condition used while patterning.^[108]

Being heat a universal stimulus, it can be used to pattern a huge variety of materials presenting different functional and structural properties. In addition to phase change and 2D materials, thermal scanning probe lithography and direct laser writing have been in fact employed to fabricate, for instance, ferroelectric and superconducting nanostructures. In Figure 5e,f two applications of tSPL are reported, where the patterns have been obtained by localized heating from a hot AFM tip on a ferroelectric material. The first one shows a crystallized line pattern

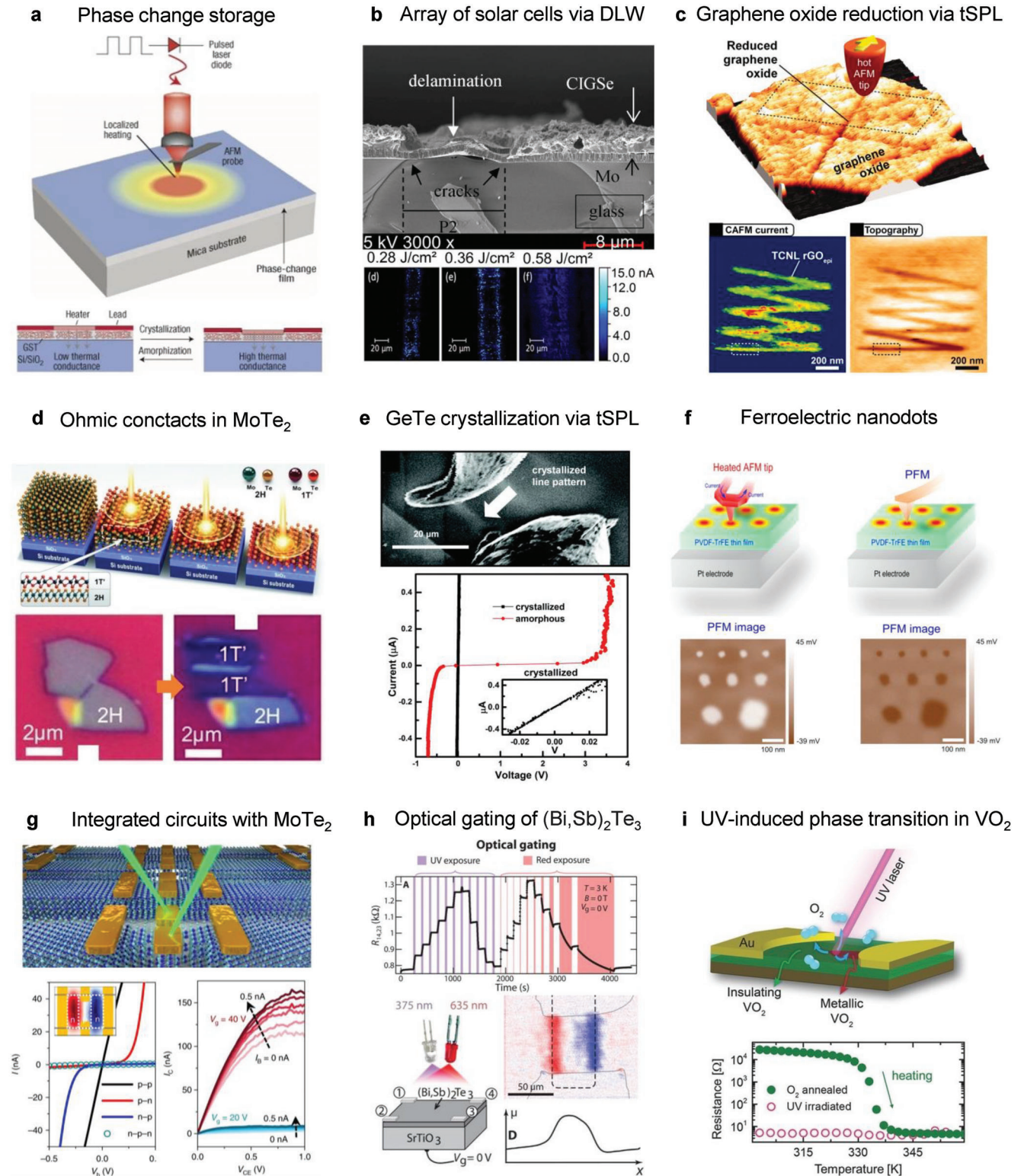


Figure 5. Applications in nanoelectronics. a) Crystallization and amorphization of GST films via tSPL for thermal phase change storage. Adapted with permission.^[96] Copyright 2006, Springer Nature. b) Laser exposure tunes the electrical conductivity of CIGSe channels for serial connections of solar cells. Adapted with permission.^[99] Copyright 2016, Elsevier. c) Nanoscale reduction of graphene oxide via tSPL; patterned areas show a much larger electrical conductivity. Adapted with permission.^[101] American Association for the Advancement of Science. d) Focused light induces a phase change in few-layer MoTe₂, allowing ohmic homojunction contacts for 2D electronics. Adapted with permission.^[105] American Association for the Advancement of Science. e) Phase nanoengineering of a GeTe film via tSPL produces a change in the conduction properties. Adapted with permission.^[109] Copyright

on amorphous GeTe having different morphological, optical, and electronic behavior,^[109] while in the second one different-sized ferroelectric dots are measured by PFM after being patterned on poly(vinylidene fluoride-ran-trifluoroethylene).^[110]

A different phenomenon which can be induced via DLW is the so-called optical doping (or gating). As an example, a scanning light probe was used in order to induce charge doping in the aforementioned TMDC MoTe₂.^[111] Here, as pointed out by the experimental data in Figure 5g, laser light impinging on metal patterns fabricated over channels of (2H)MoTe₂ can convert them from an n-type to a p-type semiconductor, resulting in a monolithic integrated circuit based on a 2D semiconducting material. Moreover, optical gating by means of UV and red laser light irradiation was successfully employed to persistently locally tune the chemical potential of thin films of the topological insulator (Bi,Sb)₂Te₃ grown on SrTiO₃ (Figure 5h).^[112,113] Optical gating appears to be equivalent to conventional electrostatic gating, but it does not require additional lithographic steps and deposition of material, promoting further studies on topological insulators and their application in quantum computing and spintronics.

Exposure to focalized UV light can also induce effects that are not directly thermally activated, as in the case of the patterning of confined conductive conduits into the otherwise insulating VO₂, a strongly correlated material widely studied for its metal-to-insulator (MIT) phase transition.^[114] Figure 5i shows the large resistivity drop of irradiated VO₂ areas and a sketch of the technique. Given a minimum energy threshold to activate the process, it is hence possible to employ shorter UV wavelength to achieve narrower features and higher resolution, and/or combine heat and UV light in order to obtain complex structures showing different optical and electronic properties.

One of the main advantages of tSPL and DLW is the possibility of single-step patterning and creating structures with different electronic properties starting with a layer of a single material. However, it is worth mentioning a slightly different approach, consisting on the activation of a process involving different structures or materials already deposited on the same sample. This is the case, for instance, of crafting the microstructure of perovskite films, which nowadays remains a critical task for high-performance optoelectronics. In this context, it was recently shown that by scanning a pulsed laser over carbon quantum dots implanted into a perovskite thin film, the resulting grain boundaries are much larger than those following standard thermal annealing, yielding enhanced crystallinity and phase stability.^[115]

Thermal scanning probe lithography and direct laser writing are extremely versatile techniques for patterning nanostructures on different materials. On the other hand, although a lot of effort has been done in order to increase the throughput and minimum feature size of SPL,^[116] optical lithography, particularly extreme UV lithography (EUVL), are far from being reached in terms of joint resolution and large scale production when deal-

ing with electronic devices. Even so, in the recent years the interest raised by the observation of exotic electronic properties in quantum materials seeks new strategies in nanofabrication which go beyond conventional processes as a matter of tunability and compatibility for the exploitation of advanced features in next-generation electronics.^[117,118] Phase nanoengineering, with the aim of crafting thoroughly the physical and structural properties of low-dimensional system, represents a key viable route in this regard. Particularly, it is promising for patterning periodic and arbitrarily-shaped grayscale (i.e., 3D) energy landscapes for controlling the electronic properties, for fabricating electronic devices based on 2D materials,^[119] and for moving toward 3D nanostructuring.^[120] To sum up, while remaining mostly a technique suitable for scientific research and niche production, tSPL and DLW can pave the way to the comprehension and harnessing of uncharted electronic properties and materials, and ultimately devising new electronical components.

5. Conclusions

Direct modification of materials encompasses a huge variety of systems and techniques, and exploits a wide range of physicochemical phenomena. In this paper, we gave an outlook on phase nanoengineering and other approaches for directly modifying the materials properties, with applications in nanomagnetism, photonics, and electronics. In this framework, thermal scanning probe lithography and direct laser writing allow the unique opportunity to deliver energy to the system, without any unwanted effect associated with charges or particles. This provides enhanced capabilities in terms of tunability and flexibility which are not achievable with conventional nanofabrication techniques, and is therefore an extremely promising field of research.

In the field of magnetism, the capability of tuning the magnetic properties with nanoscale resolution is a key feature in the development of spintronic devices. An example is the patterning of spin textures, which can be used both as information carriers or as a magnetic potential landscape to control spin waves. Computing platforms based on Boolean and non-Boolean approaches, devices for signal processing and sensors are few examples of possible applications. In photonics, phase nanoengineering applied to phase change materials (PCMs) allows the modulation of fundamental optical properties such as refractive indices and absorption coefficients. In addition, the presence of intermediate crystalline phases can be exploited to obtain complex nonlinear optical states. Different applications, such as computing, fabrication of optical elements, and information encryption can be envisaged. In the framework of beyond CMOS computing and flexible electronics, 2D materials and PCMs have been extensively studied. The tuning of their resistivity via phase nanoengineering can be employed in view of creating monolithic interconnections, data storage devices, transistors. Beyond the

2017, Royal Society of Chemistry. f) Patterning of ferroelectric nanodots based on tSPL and measured by PFM. Adapted with permission.^[110] Copyright 2013, American Chemical Society. g) Integrated electronic circuits based on MoTe₂ doping fabricated by laser irradiation. Adapted with permission.^[111] Copyright 2018, Springer Nature. h) DLW gives optical doping in (Bi,Sb)₂Te₃ by locally varying the chemical potential. Adapted with permission.^[112] Copyright 2015, American Association for the Advancement of Science. i) Metallic regions result from UV laser patterning on insulating VO₂. Adapted with permission.^[114] Copyright 2016, Wiley-VCH GmbH.

mentioned examples, the variety of materials employed in electronics, from superconductors, ferroelectrics, to perovskites allows to envision the application of phase nanoengineering to different systems, to implement advanced functionalities in next generation devices.

However, several outstanding challenges lay ahead regarding both the further development of the phase-nanoengineering methodology and related techniques. Among these, reaching higher interface temperature in tSPL on thermally conductive samples, without sacrificing spatial resolution is among the most desired capabilities, as it would allow to access a whole new range of phase transitions occurring at higher thresholds, significantly extending the applicability of phase nanoengineering to other systems. Several strategies are being studied including improving the heat transfer between tip and sample in tSPL by engineering the cantilever and tip geometry and doping profiles, or moving toward materials with higher thermal stability and melting point than Si for tip fabrication, which would allow to reach higher heater temperatures. Regarding DWL, increasing spatial resolution below the diffraction limit represents a key goal for approaching length scales in the deep sub-100 nm range, which would make DWL phase nanoengineering appealing for nanoelectronic applications. In this sense, super-resolution lithography techniques such as near-field optical techniques^[121] or plasmon lithography^[122] represent viable approaches for reaching sub-diffraction spatial resolution patterning, and could be employed for phase nanoengineering.

Regarding applications, phase nanoengineering features a unique set of capabilities appealing for device fabrication and industry, such as the possibility to self-align and overlay to previous patterns derived from in situ reading capabilities of tSPL, and the fact that direct writing allows minimal disruption to the unpatterned material. Furthermore, the possibility to confine the energy transfer in three-dimensions, for example, on the surface of the material in case of tSPL and within the volume of the material in case of DWL, allows to envision the application of phase nanoengineering for the fabrication of 3D nanostructures. Such patterning capabilities are extremely sought for the design of 3D monolithic devices in both nanoelectronics and nanophotonics. However, the fundamental limitations of serial patterning methodologies (see Section 3.3), which have prevented so far their widespread application hold true also for phase nanoengineering. In this framework, at least in the short-medium term, it can be envisioned that the unique capabilities of phase nanoengineering can be employed within multistep processes, for carrying out specific tasks which cannot be achieved via conventional nanofabrication. In this framework, the adoption of phase nanoengineering outside research labs will ultimately depend on the scalability of the process and ease of integration with conventional processes and materials.

In summary, phase nanoengineering of condensed matter allows the realization of a new class of materials and devices, where new physics and functions emerge as a result of the coexistence and interaction of different structural, electronic, or magnetic phases, at the nanoscale. While both tSPL and DWL are mature technologies, their application to the direct modification of the physical properties of condensed matter systems is rather recent and offers extremely interesting perspectives due to its wide applicability and unique capabilities. This opens new possibilities to

induce, study, and harness novel physical phenomena in a wide range of technologically relevant systems.

Acknowledgements

V.L. and D.G. contributed equally to this work. This work was partially performed at PoliFAB, the microtechnology and nanotechnology center of the Politecnico di Milano. The research leading to these results has received funding from the European Union's Horizon 2020 research and innovation programme under grant agreement number 948225 (project B3YOND). This work has been supported by the FARE programme of the Italian Ministry for University and Research (MUR) under grant agreement R20FC3PX8R (project NAMASTE). This work has been supported by Fondazione Cariplo and Fondazione CDP, grant no. 2022-1881.

Conflict of Interest

The authors declare no conflict of interest.

Keywords

laser lithography, magnonics, nanoelectronics, nanofabrication, nanomagnetism, nanomaterial, nanooptics, phase change material, thermal nanolithography

Received: February 3, 2023

Revised: April 21, 2023

Published online: May 23, 2023

- [1] *Handbook of Thin Film Deposition*, 4th ed., William Andrew Publishing, Norwich, NY 2018.
- [2] X. Liu, M. C. Hersam, *Nat. Rev. Mater.* **2019**, *4*, 669.
- [3] *Nat. Phys.* **2016**, *12*, 105.
- [4] *Fundamentals of Microfabrication and Nanotechnology, Three-Volume Set*, <https://www.routledge.com/Fundamentals-of-Microfabrication-and-Nanotechnology-Three-Volume-Set/Madou/p/book/9780849331800> (accessed: May 2023).
- [5] W. Cai, V. Shalaev, *Optical Metamaterials*, Springer, New York, NY 2010.
- [6] A. V. Chumak, A. A. Serga, B. Hillebrands, *J. Phys. D: Appl. Phys.* **2017**, *50*, 244001.
- [7] *Photonic Crystals* (Eds: K. Inoue, K. Ohtaka), Springer, Berlin, Heidelberg 2004.
- [8] E. Albisetti, D. Petti, G. Sala, R. Silvani, S. Tacchi, S. Finizio, S. Wintz, A. Calò, X. Zheng, J. Raabe, E. Riedo, R. Bertacco, *Commun. Phys.* **2018**, *1*, 56.
- [9] E. Albisetti, S. Tacchi, R. Silvani, G. Scaramuzzi, S. Finizio, S. Wintz, C. Rinaldi, M. Cantoni, J. Raabe, G. Carlotti, R. Bertacco, E. Riedo, D. Petti, *Adv. Mater.* **2020**, *32*, 1906439.
- [10] C. S. Lee, B. Jankó, I. Derényi, A. L. Barabási, *Nature* **1999**, *400*, 337.
- [11] E. Albisetti, A. Calò, A. Zanut, X. Zheng, G. M. de Peppo, E. Riedo, *Nat. Rev. Methods Primers* **2022**, *2*, 32.
- [12] S. T. Howell, A. Grushina, F. Holzner, J. Brugger, *Microsyst. Nanoeng.* **2020**, *6*, 21.
- [13] S. C. Singh, H. B. Zeng, C. Guo, W. Cai, *Nanomaterials: Processing and Characterization with Lasers*, John Wiley & Sons, Hoboken, NJ 2012.
- [14] R. Garcia, A. W. Knoll, E. Riedo, *Nat. Nanotechnol.* **2014**, *9*, 577.
- [15] D. Pires, J. L. Hedrick, A. De Silva, J. Frommer, B. Gotsmann, H. Wolf, M. Despont, U. Duerig, A. W. Knoll, *Science* **2010**, *328*, 732.

- [16] A. W. Knoll, D. Pires, O. Coulembier, P. Dubois, J. L. Hedrick, J. Frommer, U. Duerig, *Adv. Mater.* **2010**, *22*, 3361.
- [17] R. Szoszkiewicz, T. Okada, S. C. Jones, T. D. Li, W. P. King, S. R. Marder, E. Riedo, *Nano Lett.* **2007**, *7*, 1064.
- [18] K. M. Carroll, A. J. Giordano, D. Wang, V. K. Kodali, J. Scrimgeour, W. P. King, S. R. Marder, E. Riedo, J. E. Curtis, *Langmuir* **2013**, *29*, 8675.
- [19] E. Albisetti, D. Petti, M. Pancaldi, M. Madami, S. Tacchi, J. Curtis, W. P. King, A. Papp, G. Csaba, W. Porod, P. Vavassori, E. Riedo, R. Bertacco, *Nat. Nanotechnol.* **2016**, *11*, 545.
- [20] C. M. Schwarz, S. M. Kuebler, C. Rivero-Baleine, B. Triplett, M. Kang, Q. Altemose, C. Blanco, K. A. Richardson, Q. Du, S. Deckoff-Jones, J. Hu, Y. Zhang, Y. Pan, C. Ríos, *J. Opt. Microsyst.* **2021**, *1*, 013502.
- [21] P. C. Paul, A. W. Knoll, F. Holzner, M. Despont, U. Duerig, *Nanotechnology* **2011**, *22*, 275306.
- [22] P. C. Paul, in *Frontiers of Nanoscience*, Elsevier, Amsterdam **2016**, pp. 543–561.
- [23] F. Holzner, P. Paul, M. Despont, L. L. Cheong, J. Hedrick, U. Dürig, A. Knoll, in *29th European Mask and Lithography Conf.*, SPIE, Dresden, Germany **2013**, p. 26.
- [24] A. W. Knoll, M. Zientek, L. L. Cheong, C. Rawlings, P. Paul, F. Holzner, J. L. Hedrick, D. J. Coady, R. Allen, U. Dürig, in *Alternative Lithographic Technologies VI*, SPIE, San Jose, CA **2014**, p. 47.
- [25] X. Zheng, A. Calò, E. Albisetti, X. Liu, A. S. M. Alharbi, G. Arefe, X. Liu, M. Spieser, W. J. Yoo, T. Taniguchi, K. Watanabe, C. Aruta, A. Ciarrocchi, A. Kis, B. S. Lee, M. Lipson, J. Hone, D. Shahrjerdi, E. Riedo, *Nat. Electron.* **2019**, *2*, 17.
- [26] M. Spieser, C. Rawlings, E. Lörtscher, U. Duerig, A. W. Knoll, *J. Appl. Phys.* **2017**, *121*, 174503.
- [27] B. Nelson, W. King, *Nanoscale Microscale Thermophys. Eng.* **2008**, *12*, 98.
- [28] M. Duocastella, C. Florian, P. Serra, A. Diaspro, *Sci. Rep.* **2015**, *5*, 16199.
- [29] Z. L. Wu, Y. N. Qi, X. J. Yin, X. Yang, C. M. Chen, J. Y. Yu, J. C. Yu, Y. M. Lin, F. Hui, P. L. Liu, Y. X. Liang, Y. Zhang, M. S. Zhao, *Polymers* **2019**, *11*, 553.
- [30] A. Selimis, V. Mironov, M. Farsari, *Microelectron. Eng.* **2015**, *132*, 83.
- [31] Y. C. Chan, *Opt. Eng.* **1998**, *37*, 2521.
- [32] S. Somnath, H. J. Kim, H. Hu, W. P. King, *Nanotechnology* **2013**, *25*, 014001.
- [33] K. M. Carroll, X. Lu, S. Kim, Y. Gao, H. J. Kim, S. Somnath, L. Polloni, R. Sordan, W. P. King, J. E. Curtis, E. Riedo, *Nanoscale* **2014**, *6*, 1299.
- [34] J. Wang, Q. Zhang, Y. Yan, Y. Liu, Y. Geng, *Appl. Surf. Sci.* **2022**, *576*, 151790.
- [35] L. Yang, A. El-Tamer, U. Hinze, J. Li, Y. Hu, W. Huang, J. Chu, B. N. Chichkov, *Opt. Lasers Eng.* **2015**, *70*, 26.
- [36] D. Weber, R. Heimbürger, D. Hildebrand, T. Junghans, G. Schondelmaier, C. Walther, D. Schondelmaier, *Appl. Phys. A* **2019**, *125*, 307.
- [37] H. Wolf, Y. K. R. Cho, S. Karg, P. Mensch, C. Schwemmer, A. Knoll, M. Spieser, S. Bisig, C. Rawlings, P. Paul, F. Holzner, U. Duerig, in *2019 Pan Pacific Microelectronics Symposium (Pan Pacific)*, IEEE, Kauai, HI, USA **2019**, pp. 1–9.
- [38] E. Y. Vedmedenko, R. K. Kawakami, D. D. Sheka, P. Gambardella, A. Kirilyuk, A. Hirohata, C. Binek, O. Chubykalo-Fesenko, S. Sanvito, B. J. Kirby, J. Grollier, K. Everschor-Sitte, T. Kampfrath, C. Y. You, A. Berger, *J. Phys. D: Appl. Phys.* **2020**, *53*, 453001.
- [39] J. Nogués, I. K. Schuller, *J. Magn. Magn. Mater.* **1999**, *192*, 203.
- [40] E. Albisetti, D. Petti, *J. Magn. Magn. Mater.* **2016**, *400*, 230.
- [41] E. Albisetti, A. Calò, M. Spieser, A. W. Knoll, E. Riedo, D. Petti, *Appl. Phys. Lett.* **2018**, *113*, 162401.
- [42] Z. R. Yan, Y. Z. Liu, Y. Guang, J. F. Feng, R. K. Lake, G. Q. Yu, X. F. Han, *Phys. Rev. Appl.* **2020**, *14*, 044008.
- [43] D. Petti, S. Tacchi, E. Albisetti, *J. Phys. D: Appl. Phys.* **2022**, *55*, 293003.
- [44] A. Barman, G. Gubbiotti, S. Ladak, A. O. Adeyeye, M. Krawczyk, J. Gräfe, C. Adelman, S. Cotofana, A. Naeemi, V. I. Vasyuchka, B. Hillebrands, S. A. Nikitov, H. Yu, D. Grundler, A. V. Sadovnikov, A. A. Grachev, S. E. Sheshukova, J. Y. Duquesne, M. Marangolo, G. Csaba, W. Porod, V. E. Demidov, S. Urazhdin, S. O. Demokritov, E. Albisetti, D. Petti, R. Bertacco, H. Schultheiss, V. V. Kruglyak, V. D. Poimanov, et al., *J. Phys.: Condens. Matter* **2021**, *33*, 413001.
- [45] P. Pirro, V. I. Vasyuchka, A. A. Serga, B. Hillebrands, *Nat. Rev. Mater.* **2021**, *6*, 1114.
- [46] Y. K. Ryu, A. W. Knoll, in *Electrical Atomic Force Microscopy for Nanoelectronics* (Ed.: U. Celano), Springer International Publishing, Cham **2019**, pp. 143–172.
- [47] H. W. Shin, J. Y. Son, *Mater. Lett.* **2018**, *213*, 331.
- [48] A. Kirilyuk, A. V. Kimel, T. Rasing, *Spintronics Handbook, Second Edition: Spin Transport and Magnetism*, CRC Press, Boca Raton, FL **2019**.
- [49] A. M. Alekseev, Yu. K. Verevkin, N. V. Vostokov, V. N. Petryakov, N. I. Polushkin, A. F. Popkov, N. N. Salashchenko, *JETP Lett.* **2001**, *73*, 192.
- [50] J. Kisielewski, W. Dobrogowski, Z. Kurant, A. Stupakiewicz, M. Tekielak, A. Kirilyuk, A. Kimel, Th. Rasing, L. T. Baczewski, A. Wawro, K. Balin, J. Szade, A. Maziewski, *J. Appl. Phys.* **2014**, *115*, 053906.
- [51] J. Kisielewski, K. Postava, I. Sveklo, A. Nedzved, P. Trzcinski, A. Maziewski, B. Szymański, M. Urbaniak, F. Stobiecki, *Solid State Phenomena* **2008**, *140*, 69.
- [52] M. Vogel, A. V. Chumak, E. H. Waller, T. Langner, V. I. Vasyuchka, B. Hillebrands, G. von Freymann, *Nat. Phys.* **2015**, *11*, 487.
- [53] A. A. Serga, A. V. Chumak, B. Hillebrands, *J. Phys. D: Appl. Phys.* **2010**, *43*, 264002.
- [54] S. Daimon, R. Iguchi, K. Uchida, E. Saitoh, *J. Phys. D: Appl. Phys.* **2015**, *48*, 164014.
- [55] Q. Wang, A. V. Chumak, P. Pirro, *Nat. Commun.* **2021**, *12*, 2636.
- [56] A. Papp, W. Porod, G. Csaba, *Nat. Commun.* **2021**, *12*, 6422.
- [57] S. H. Skjærø, C. H. Marrows, R. L. Stamps, L. J. Heyderman, *Nat. Rev. Phys.* **2020**, *2*, 13.
- [58] S. Lendinez, M. B. Jungfleisch, *J. Phys.: Condens. Matter* **2019**, *32*, 013001.
- [59] J. C. Gartside, K. D. Stenning, A. Vanstone, H. H. Holder, D. M. Arroyo, T. Dion, F. Caravelli, H. Kurebayashi, W. R. Branford, *Nat. Nanotechnol.* **2022**, *17*, 460.
- [60] N. Sisodia, J. Pelloux-Prayer, L. D. Buda-Prejbeanu, L. Anghel, G. Gaudin, O. Boulle, *Phys. Rev. Appl.* **2022**, *17*, 064035.
- [61] N. Sisodia, J. Pelloux-Prayer, L. D. Buda-Prejbeanu, L. Anghel, G. Gaudin, O. Boulle, *Phys. Rev. Appl.* **2022**, *18*, 014025.
- [62] Z. Luo, A. Hrabec, T. P. Dao, G. Sala, S. Finizio, J. Feng, S. Mayr, J. Raabe, P. Gambardella, L. J. Heyderman, *Nature* **2020**, *579*, 214.
- [63] M. Gibertini, M. Koperski, A. F. Morpurgo, K. S. Novoselov, *Nat. Nanotechnol.* **2019**, *14*, 408.
- [64] E. Elahi, G. Dastgeer, G. Nazir, S. Nisar, M. Bashir, H. Akhter Qureshi, D. Kim, J. Aziz, M. Aslam, K. Hussain, M. A. Assiri, M. Imran, *Comput. Mater. Sci.* **2022**, *213*, 111670.
- [65] *Femtosecond Laser Micromachining: Photonic and Microfluidic Devices in Transparent Materials* (Eds: R. Osellame, G. Cerullo, R. Ramponi), Springer, Berlin, Heidelberg **2012**.
- [66] R. R. Gattass, E. Mazur, *Nat. Photonics* **2008**, *2*, 219.
- [67] J. Wang, L. Wang, J. Liu, *IEEE Access* **2020**, *8*, 121211.
- [68] W. Zhang, R. Mazzarello, E. Ma, *MRS Bull.* **2019**, *44*, 686.
- [69] A. Mandal, Y. Cui, L. McRae, B. Gholipour, *J. Phys. Photonics* **2021**, *3*, 022005.
- [70] G. Bakan, S. Ayas, E. Ozgur, K. Celebi, A. Dana, *ACS Sens.* **2016**, *1*, 1403.
- [71] X. Wang, H. Qi, X. Hu, Z. Yu, S. Ding, Z. Du, Q. Gong, *Molecules* **2021**, *26*, 2813.

- [72] M. Wuttig, N. Yamada, *Nat. Mater.* **2007**, *6*, 824.
- [73] M. Rudé, J. Pello, R. E. Simpson, J. Osmond, G. Roelkens, J. J. G. M. van der Tol, V. Pruneri, *Appl. Phys. Lett.* **2013**, *103*, 141119.
- [74] C. Wu, H. Yu, H. Li, X. Zhang, I. Takeuchi, M. Li, *ACS Photonics* **2019**, *6*, 87.
- [75] Z. Cheng, C. Ríos, N. Youngblood, C. D. Wright, W. H. P. Pernice, H. Bhaskaran, *Adv. Mater.* **2018**, *30*, 1802435.
- [76] C. Ríos, P. Hosseini, C. D. Wright, H. Bhaskaran, W. H. P. Pernice, *Adv. Mater.* **2014**, *26*, 1372.
- [77] C. Wu, H. Yu, S. Lee, R. Peng, I. Takeuchi, M. Li, *Nat. Commun.* **2021**, *12*, 96.
- [78] I. Chakraborty, G. Saha, K. Roy, *Phys. Rev. Appl.* **2019**, *11*, 014063.
- [79] F. Brücknerhoff-Plückelmann, J. Feldmann, C. D. Wright, H. Bhaskaran, W. H. P. Pernice, *J. Appl. Phys.* **2021**, *129*, 151103.
- [80] U. Cataldi, R. Caputo, Y. Kurylyak, G. Klein, M. Chekini, C. Umetsu, T. Bürgi, *J. Mater. Chem. C* **2014**, *2*, 7927.
- [81] I. C. Khoo, J. H. Park, J. D. Liou, *J. Opt. Soc. Am. B* **2008**, *25*, 1931.
- [82] M. Y. Shalaginov, S. An, Y. Zhang, F. Yang, P. Su, V. Liberman, J. B. Chou, C. M. Roberts, M. Kang, C. Ríos, Q. Du, C. Fowler, A. Agarwal, K. A. Richardson, C. Rivero-Baleine, H. Zhang, J. Hu, T. Gu, *Nat. Commun.* **2021**, *12*, 1225.
- [83] P. Hosseini, C. D. Wright, H. Bhaskaran, *Nature* **2014**, *511*, 206.
- [84] W. Dong, H. Liu, J. K. Behera, L. Lu, R. J. H. Ng, K. V. Sreekanth, X. Zhou, J. K. W. Yang, R. E. Simpson, *Adv. Funct. Mater.* **2019**, *29*, 1806181.
- [85] K. V. Sreekanth, S. Han, R. Singh, *Adv. Mater.* **2018**, *30*, 1706696.
- [86] Q. Wang, E. T. F. Rogers, B. Gholipour, C. M. Wang, G. Yuan, J. Teng, N. I. Zheludev, *Nat. Photonics* **2016**, *10*, 60.
- [87] C. R. de Galarreta, A. M. Alexeev, Y. Y. Au, M. Lopez-Garcia, M. Klemm, M. Cryan, J. Bertolotti, C. D. Wright, *Adv. Funct. Mater.* **2018**, *28*, 1704993.
- [88] O. A. M. Abdelraouf, Z. Wang, H. Liu, Z. Dong, Q. Wang, M. Ye, X. R. Wang, Q. J. Wang, H. Liu, *ACS Nano* **2022**, *16*, 13339.
- [89] F. Zhang, X. Xie, M. Pu, Y. Guo, X. Ma, X. Li, J. Luo, Q. He, H. Yu, X. Luo, *Adv. Mater.* **2020**, *32*, 1908194.
- [90] O. A. M. Abdelraouf, A. P. Anthur, Z. Dong, H. Liu, Q. Wang, L. Krivitsky, X. Renshaw Wang, Q. J. Wang, H. Liu, *Adv. Funct. Mater.* **2021**, *31*, 2104627.
- [91] Q. Zheng, Y. Wang, J. Zhu, *J. Phys. D: Appl. Phys.* **2017**, *50*, 243002.
- [92] S. Raoux, F. Xiong, M. Wuttig, E. Pop, *MRS Bull.* **2014**, *39*, 703.
- [93] W. Li, X. Qian, J. Li, *Nat. Rev. Mater.* **2021**, *6*, 829.
- [94] S. Manzeli, D. Ovchinnikov, D. Pasquier, O. V. Yazyev, A. Kis, *Nat. Rev. Mater.* **2017**, *2*, 17033.
- [95] C. H. Chu, C. D. Shiue, H. W. Cheng, M. L. Tseng, H. P. Chiang, M. Mansuripur, D. P. Tsai, *Opt. Express* **2010**, *18*, 18383.
- [96] H. F. Hamann, M. O'Boyle, Y. C. Martin, M. Rooks, H. K. Wickramasinghe, *Nat. Mater.* **2006**, *5*, 383.
- [97] A. Dun, J. Wei, F. Gan, *Thin Solid Films* **2011**, *519*, 3859.
- [98] Y. Zhang, L. Liu, G. Zou, N. Chen, A. Wu, H. Bai, Y. Zhou, *J. Appl. Phys.* **2015**, *117*, 023109.
- [99] C. Schultz, M. Schuele, K. Stelmaszczyk, M. Weizman, O. Gref, F. Friedrich, C. Wolf, N. Papanthanasios, C. A. Kaufmann, B. Rau, R. Schlattmann, V. Quaschnig, F. Fink, B. Stegemann, *Sol. Energy Mater. Sol. Cells* **2016**, *157*, 636.
- [100] S. Raghuraman, M. B. Eliński, J. D. Batteas, J. R. Felts, *Nano Lett.* **2017**, *17*, 2111.
- [101] Z. Wei, D. Wang, S. Kim, S. Y. Kim, Y. Hu, M. K. Yakes, A. R. Laracuente, Z. Dai, S. R. Marder, C. Berger, W. P. King, W. A. de Heer, P. E. Sheehan, E. Riedo, *Science* **2010**, *328*, 1373.
- [102] W. K. Lee, M. Haydell, J. T. Robinson, A. R. Laracuente, E. Cimpoiu, W. P. King, P. E. Sheehan, *ACS Nano* **2013**, *7*, 6219.
- [103] Y. Tan, F. Luo, M. Zhu, X. Xu, Y. Ye, B. Li, G. Wang, W. Luo, X. Zheng, N. Wu, Y. Yu, S. Qin, X. A. Zhang, *Nanoscale* **2018**, *10*, 19964.
- [104] M. Wang, D. Li, K. Liu, Q. Guo, S. Wang, X. Li, *ACS Nano* **2020**, *14*, 11169.
- [105] S. Cho, S. Kim, J. H. Kim, J. Zhao, J. Seok, D. H. Keum, J. Baik, D. H. Choe, K. J. Chang, K. Suenaga, S. W. Kim, Y. H. Lee, H. Yang, *Science* **2015**, *349*, 625.
- [106] S. Kim, J. H. Kim, D. Kim, G. Hwang, J. Baik, H. Yang, S. Cho, *2D Mater.* **2017**, *4*, 024004.
- [107] N. Papadopoulos, J. O. Island, H. S. J. van der Zant, G. A. Steele, *IEEE Trans. Electron Devices* **2018**, *65*, 4053.
- [108] X. Zheng, A. Calò, T. Cao, X. Liu, Z. Huang, P. M. Das, M. Drndić, E. Albisetti, F. Lavini, T. D. Li, V. Narang, W. P. King, J. W. Harrold, M. Vittadello, C. Aruta, D. Shahrjerdi, E. Riedo, *Nat. Commun.* **2020**, *11*, 3463.
- [109] A. Podpirka, W. K. Lee, J. I. Ziegler, T. H. Brintlinger, J. R. Felts, B. S. Simpkins, N. D. Bassim, A. R. Laracuente, P. E. Sheehan, L. B. Ruppalt, *Nanoscale* **2017**, *9*, 8815.
- [110] J. Y. Son, I. Jung, Y. H. Shin, *J. Phys. Chem. C* **2013**, *117*, 12890.
- [111] S. Y. Seo, J. Park, J. Park, K. Song, S. Cha, S. Sim, S. Y. Choi, H. W. Yeom, H. Choi, M. H. Jo, *Nat. Electron.* **2018**, *1*, 512.
- [112] A. L. Yeats, Y. Pan, A. Richardella, P. J. Mintun, N. Samarth, D. D. Awschalom, *Sci. Adv.* **2015**, *1*, e1500640.
- [113] A. L. Yeats, P. J. Mintun, Y. Pan, A. Richardella, B. B. Buckley, N. Samarth, D. D. Awschalom, *Proc. Natl. Acad. Sci. U. S. A.* **2017**, *114*, 10379.
- [114] H. Zhang, L. Guo, G. Stone, L. Zhang, Y. Zheng, E. Freeman, D. W. Keefer, S. Chaudhuri, H. Paik, J. A. Moyer, M. Barth, D. G. Schlom, J. V. Badding, S. Datta, V. Gopalan, R. Engel-Herbert, *Adv. Funct. Mater.* **2016**, *26*, 6612.
- [115] C. Song, H. Yang, F. Liu, L. Ye, G. J. Cheng, *Adv. Mater. Interfaces* **2020**, *7*, 2001021.
- [116] P. Fan, J. Gao, H. Mao, Y. Geng, Y. Yan, Y. Wang, S. Goel, X. Luo, *Micromachines* **2022**, *13*, 228.
- [117] J. T. Fourkas, J. Gao, Z. Han, H. Liu, B. Marmiroli, M. J. Naughton, J. S. Petersen, Y. Sun, A. V. Pret, Y. Zheng, *Front. Nanotechnol.* **2021**, *3*, 700849.
- [118] R. Bertacco, G. Panaccione, S. Picozzi, *Materials* **2022**, *15*, 4478.
- [119] S. Liu, J. Wang, J. Shao, D. Ouyang, W. Zhang, S. Liu, Y. Li, T. Zhai, *Adv. Mater.* **2022**, *34*, 2200734.
- [120] G. Seniutinas, A. Balčytis, I. Reklaitis, F. Chen, J. Davis, C. David, S. Juodkazis, *Nanophotonics* **2017**, *6*, 923.
- [121] A. A. Tseng, *Opt. Laser Technol.* **2007**, *39*, 514.
- [122] F. Hong, R. Blaikie, *Adv. Opt. Mater.* **2019**, *7*, 1801653.